

Kinetic Phenomena in Spherical Expanding Flows of Binary Gas Mixtures

Vladimir V. Riabov*

Rivier College, Nashua, New Hampshire 03060

Diffusion and kinetic effects in the spherical expanding flows of argon–helium mixtures have been studied using the direct simulation Monte Carlo technique at the Knudsen numbers from 0.0015 to 0.03 and pressure ratios from 100 to 10,000. Similarity analysis was used to analyze the flow structure in supersonic flow region, spherical shock wave, and subsonic area behind it. Both kinetic and diffusion effects influence the shock-wave thickness, parallel and transverse species temperatures, diffusion velocities, the effectiveness of species separation, and ambient gas penetration. In the supersonic region the effect of “freezing” the parallel temperature has been found in all considered cases. The temperature freezing comes first for heavier molecules of argon. The transverse temperature for both species follows the temperature in the isentropic expansion. Accumulation of the hot light (helium) component occurs in the leading front of the spherical shock wave. The multitemperature regime of the flow inside the shock wave is found and studied using the similarity factor, which is based on the ratio of stagnation pressures calculated at critical-source-flow and background conditions.

Nomenclature

C	= constant; Eq. (5)
F	= transformed mole-fraction function; Eq. (15)
f	= mole fraction of heavier component
H	= transformed temperature function; Eq. (15)
Kn_a	= Knudsen number based on the length scale parameter at infinity L
Kn_*	= Knudsen number based on the critical radius of a spherical source r_*
K_2	= similarity parameter, $Re_*(p_a/p_{0*})^{1/2}$
k	= Boltzmann constant, 1.380658×10^{-23} J/K
L	= length scale parameter at infinity, $[QU_a/(4\pi\gamma p_a)]^{1/2}$, m
M	= Mach number, u/U
m	= mass of a molecule, kg
n	= number density, $1/m^3$
P	= pressure ratio, p_{0*}/p_a
p	= pressure, N/m ²
Q	= total mass flow rate, $4\pi\rho ur^2$
R	= asymptotic parameter, $0.75Re_*$
R_a	= length scale normalization parameter behind the shock wave; Eq. (5), $r_*(p_{0*}/p_a)^{1/2}$
Re_*	= Reynolds number calculated by flow parameters at the critical sphere, $\rho_*u_*r_*/\mu_*$
r	= radius or spherical coordinate, m
r_*	= radius of spherical source, m
S	= entropy, J/kg/K
Sc	= Schmidt number
s	= exponent in the viscosity law $\mu \sim T^s$
T	= temperature, K
TTX	= parallel translational temperature, K
TTY	= transverse translational temperature, K
U	= speed of sound in the medium, m/s
u	= radial velocity component, m/s
u_0	= constant; Eqs. (10), (11), and (13)
u_1	= constant; Eq. (11)

W	= transformed velocity function; Eq. (15)
X	= transformed coordinate; Eq. (15)
x	= inverse dimensionless radius, r_*/r
β	= thermal diffusion ratio
γ	= ratio of specific heats
ε	= ratio of molecular weights, m_{He}/m_{Ar}
θ_1	= constant; Eqs. (11–13)
λ	= expansion parameter, $2\omega(\gamma - 1)$; Eq. (15)
μ	= molecular viscosity, kg/m/s
ρ	= density, kg/m ³
ϕ_*	= constant, $\varepsilon + (1 - \varepsilon)f_*$
ω	= expansion parameter, $1/[2\gamma - 1 - 2(\gamma - 1)s]$; Eq. (15)

Subscripts

a	= ambient medium parameter
dif	= diffusion parameter
0	= stagnation parameter
1	= heavy species parameter
+	= coordinate of the spherical shock wave in inviscid gas
*	= critical parameter at $M = 1$

Superscript

$'$	= dimensionless quantity relative to the parameters under sonic conditions
-----	--

Introduction

THE spherical expansion of a binary gas mixture into a flooded space can be considered as an important theoretical model¹ for studying separation processes in the axisymmetric jets. Gusev and Klimova² and Gusev et al.³ have found that at large distances from the nozzle exit the isentropic flow in a jet asymptotically approaches, along each ray starting from the center of the nozzle exit, the flow from some equivalent spherical source having an intensity that varies from ray to ray. Diffusive processes have a significant effect on the structure of a low-density gas mixture flow in underexpanded freejets.^{1,4–6} The flow of a binary gas mixture from a spherical source was studied by Skovorodko and Chekmarev,⁷ Gusev and Riabov,⁸ and Riabov⁹ by analyzing the numerical and asymptotic solutions of the Navier–Stokes equations. The phenomenon of background gas penetration into underexpanded freejets was described by Brook et al.,⁶ Skovorodko and Chekmarev,⁷ and Gusev and Riabov.⁸ The results could be used in studies of the separation of gas species and isotopes.^{10,11}

The areas of the shock waves in such flows could not be accurately studied by using the continuum equations. The kinetic approach

Received 2 January 2003; revision received 2 June 2003; accepted for publication 2 June 2003. Copyright © 2003 by Vladimir V. Riabov. Published by the American Institute of Aeronautics and Astronautics, Inc., with permission. Copies of this paper may be made for personal or internal use, on condition that the copier pay the \$10.00 per-copy fee to the Copyright Clearance Center, Inc., 222 Rosewood Drive, Danvers, MA 01923; include the code 0887-8722/03 \$10.00 in correspondence with the CCC.

*Associate Professor, Department of Mathematics and Computer Science, 424 S. Main Street; vriabov@rivier.edu. Senior Member AIAA.

should be applied in this case. The normal shock-wave structure in binary gas mixture was studied by Center,¹² Abe and Oguchi,¹³ Harnet and Muntz,¹⁴ and Bochkarev et al.¹⁵ and Bochkarev and Prikhodko.¹⁶ The direct simulation Monte Carlo (DSMC) technique was used by Bird^{17–19} to study flow with the normal shock waves. The systematic analysis of the diffusive processes in expanding flows based on the DSMC method has not been provided yet.

In the present study kinetic and diffusion effects in the spherical expanding flows of argon–helium mixtures have been studied using the DSMC technique^{19,20} at the Knudsen numbers (based on the sonic radius of the spherical source r_*) from 0.0015 to 0.03 and stagnation pressure ratios $P = p_{0*}/p_a$ from 100 to 10,000. The similarity analysis^{3,21} and analytical asymptotic techniques^{8,9} were used to study the flow structure. The objective of this study is that it presents a similarity analysis to provide important physical interpretations, which can be useful for understanding complex numerical simulation results.

Spherical Inviscid Gas Flow

At first, we consider the steady expansion of an inviscid gas mixture from a spherical source of radius r_* and sonic conditions. The Euler conservation equations⁸ can be transformed to the following system of equations:

$$u'[0.5(\gamma + 1) - 0.5(\gamma - 1)u^2] = x^{2(\gamma - 1)} \quad (1)$$

$$T' = 0.5(\gamma + 1) - 0.5(\gamma - 1)u^2 \quad (2)$$

$$f = f_* \quad (3)$$

where $x = r_*/r$ and the dependent variables of velocity u and temperature T are made dimensionless relative to their critical values at Mach number $M = 1$.

Velocity and temperature can be found from Eqs. (1) and (2) numerically, that is, by using the Newton–Raphson iterative method.^{8,9,20} Parameters of density ρ and pressure p are calculated from the mass conservation principle $\rho ur^2 = \rho_* u_* r_*^2$ and the perfect-gas law $p = nkT$. The mole fraction of a heavy component f remains constant in the flow [see Eq. (3)].

The Mach number M is

$$M = u' / \sqrt{T'} \quad (4)$$

As an example, distributions of Mach number, numerical density, and mole fraction of argon along (solid lines) the radial coordinate r at pressure ratio $P = p_{0*}/p_a = 100$ are shown in Figs. 1–3, respectively. The spherical inviscid gas flow could be separated by the coordinate³ r_+ of the spherical shock wave into two regions: supersonic flow area at $r_* < r < r_+$ and subsonic one at $r > r_+$, where

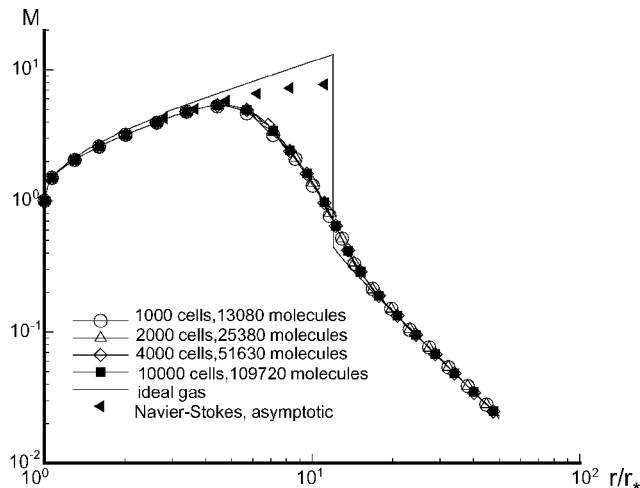


Fig. 1 Mach-number distributions in the spherical expanding flow of Ar–He mixture at $Kn_* = 0.015$ ($Re_* = 124$) and $P = 100$ for various parameter sets.

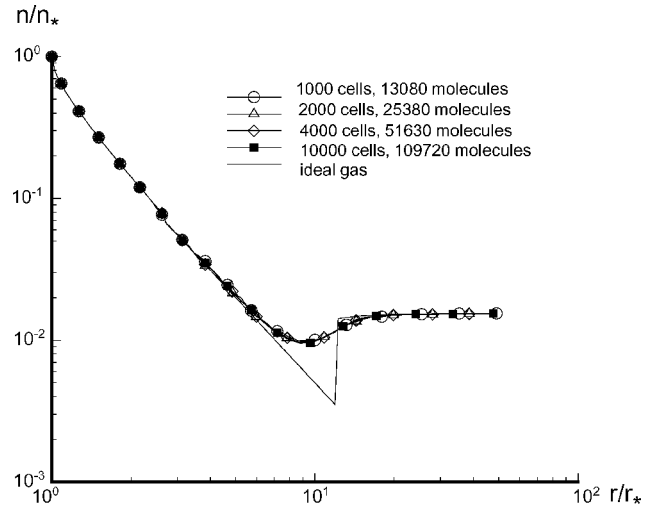


Fig. 2 Number density distributions in the spherical expanding flow of Ar–He mixture at $Kn_* = 0.015$ ($Re_* = 124$) and $P = 100$ for various parameter sets.

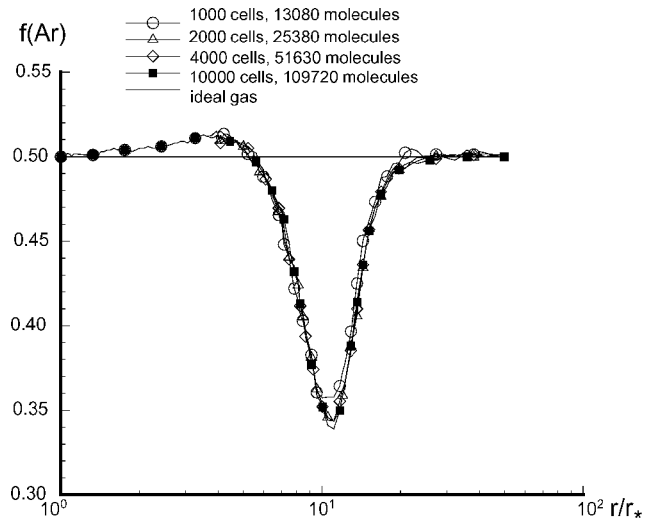


Fig. 3 Argon mole fraction distributions in the spherical expanding flow of Ar–He mixture at $Kn_* = 0.015$ ($Re_* = 124$) and $P = 100$ for the four parameter sets.

r_+ can be expressed as

$$r_+ = C R_a, \quad R_a = r_* \sqrt{\frac{p_{0*}}{p_a}} \quad (5)$$

$$C = \left(\frac{\gamma + 1}{2\gamma} \right)^{1/2(\gamma - 1)} \left(\frac{\gamma + 1}{\gamma - 1} \right)^{1/4}$$

For monatomic gas we have $\gamma = 5/3$ and $C = 1.1963$. Therefore, the main changes of flow characteristics are expected at $r \approx R_a$, which is the critical effective radius of the spherical source for the subsonic branch of the flow behind the spherical shock wave.

The ratio of total (stagnation) pressures $P = p_{0*}/p_a$ can be also used for estimating the difference of entropy across a shock wave²²:

$$S_a - S_{0*} = (k/m) \ln(p_{0*}/p_a) \quad (6)$$

Therefore, parameters R_a and P will play an important role in the study.

Transonic Inviscid Flow Solution

The solution of Eqs. (1) and (2) is singular at the sonic spherical source surface, and it cannot be used as a boundary condition in a

numerical method. In the vicinity of the point $x = 1$, the inviscid flow is transonic and can be represented by the following solution⁸ of Eqs. (1) and (2):

$$u' = 1 + \frac{2}{\sqrt{\gamma+1}}(1-x)^{0.5} + \dots \quad (7)$$

$$T' = 1 - \frac{2(\gamma-1)}{\sqrt{\gamma+1}}(1-x)^{0.5} + \dots \quad (8)$$

$$n' = \frac{x^2}{u'} \quad (9)$$

The case of transonic viscous flow near the sonic spherical source surface was considered by Gusev and Riabov⁸ and Riabov⁹ in detail.

Hypersonic Inviscid Flow Solution

For a inviscid gas flow in a hypersonic region, the following asymptotic solution^{8,9} of Eqs. (1) and (2) was found:

$$n' = \rho' = \frac{1}{u_0}x^2 + \dots, \quad u_0 = \sqrt{\frac{\gamma+1}{\gamma-1}} \quad (10)$$

$$u' = u_0 + u_1x^{2(\gamma-1)} + \dots, \quad u_1 = -\frac{\theta_1}{\sqrt{\gamma^2-1}} \quad (11)$$

$$T' = \theta_1x^{2(\gamma-1)} + \dots, \quad \theta_1 = \left(\frac{\gamma-1}{\gamma+1}\right)^{1/2(\gamma-1)} \quad (12)$$

$$p' = \frac{\theta_1}{u_0}x^{2\gamma} + \dots \quad (13)$$

where the dependent variables are made dimensionless relative to their critical values at Mach number $M = 1$.

Using Eqs. (4), (11), and (12), we can find the asymptotic solution for Mach number $M \gg 1$ along the radius of a spherical symmetric nonviscous gas flow at large distances $r \gg r_*$:

$$M = \left(\frac{\gamma+1}{\gamma-1}\right)^{(\gamma+1)/4} \left(\frac{r}{r_*}\right)^{(\gamma-1)} \quad (14)$$

Spherical Expansion of a Viscous Binary Gas Mixture

Consider the spherical expansion of a viscous binary gas mixture into a flooded space. Following the study of Chapman and Cowling,²³ the system of Navier–Stokes equations and boundary conditions were written for a one-temperature gas mixture in the case of spherical symmetry.⁸ The system of equations was solved numerically by the method developed by Gusev and Zhabkova.²⁴

The solutions⁸ obtained for density, velocity, pressure, and temperature are similar to the solutions for a one-component gas. At high Reynolds numbers Re_* the flow remains nearly nonviscous at $r < R_a$. The parameters of the mixture at $r > R_a$ correlate well with the corresponding parameters²⁵ in a one-component gas. The major difference is in the shock-wave front, where there is a considerable increase in the velocity of the light component. In the case of an argon–helium mixture ($\gamma = 5/3$, $s = 0.75$, $\varepsilon = 0.1$, $Sc = 0.333$, $Pr = 0.431$, $\beta = 0.377$, mole fraction of heavy component in flooded space $f_a = 0.5$), the maximum velocity of the helium species exceeds the limiting velocity of the mixture by a factor of 3 (Ref. 8).

The flow structure in the inner supersonic region ($r < R_a$) could be studied in terms of the asymptotic analysis.^{8,9} Here, the flow remains close to ideal. The differences become significant in the regions with the large magnitudes of function derivatives near the critical source surface and the leading front of the shock wave.

It was shown^{8,9,26} that at distances $r' = \mathcal{O}(Re_*^\omega)$ from the source in the flow dissipative and diffusive processes become important and the asymptotic solutions [see Eqs. (10–14)] are not applicable in this

region. The asymptotic solution of the Navier–Stokes equations^{8,23} in the hypersonic zone was found by Gusev and Riabov⁸ and Riabov⁹ in the case of binary mixtures. The method of deformable coordinates²⁶ was used.

The flow parameters were made dimensionless with respect to their values on the critical surface of the ideal source. These new dependent and independent variables were introduced:

$$H = T'R^\lambda, \quad W = (u' - u_0)R^\lambda, \quad F = (f - f_*)R^\lambda$$

$$X = xR^\omega, \quad \lambda = 2\omega(\gamma-1), \quad \omega = 1/[2\gamma-1-2(\gamma-1)s] \quad (15)$$

After substituting these variables into the Navier–Stokes equations and taking $R = 0.75Re_* \rightarrow \infty$, we obtain solutions of the equations^{8,9}

$$H = \left[\frac{u_0^2\gamma(\gamma-1)(1-s)}{[2\gamma-1-2s(\gamma-1)]X} + \theta_1^{1-s}X^{2(\gamma-1)(1-s)} \right]^{1/(1-s)} \quad (16)$$

$$W = -\frac{H}{u_0(\gamma-1)} - \frac{u_0H^s}{X} \quad (17)$$

$$F = \frac{3\varepsilon f_*(1-f_*)}{4Sc_*\phi_*} \left(\frac{1-\varepsilon}{\phi_*} - \beta_* \right) H^{s-1} \frac{dH}{dX} \quad (18)$$

$$\phi_* = \varepsilon + (1-\varepsilon)f_*$$

The expressions for H and W in Eqs. (16) and (17) are the same as the solutions for a one-component gas.^{25,26} Functions H and W do not contain a heavier-species mole fraction f as a parameter. As $X \rightarrow \infty$, the solution (16–18) asymptotically approaches solution (3), (11), and (12) for an ideal gas.

The result of calculations of Mach number M by using solutions (4) and (15–17) is presented in Fig. 1 (triangles) for viscous argon–helium mixture at Reynolds number $Re_* = 124$ (Knudsen number $Kn_* = 0.015$) and mole fraction of heavy component $f_* = 0.5$.

DSMC Method

The DSMC method^{19,27} and code¹⁹ (modified for flows with spherical symmetry) have been used in this study of spherical low-density binary gas mixture flows. Molecular collisions in the argon–helium mixture are modeled using the variable-hard-sphere (VHS) molecular model.^{19,27}

The inner boundary conditions for mole fraction of argon f , velocity u , temperature T , and number density n have matched the transonic continuum solutions at $r/r_* = 1.05$ [see Eqs. (3) and (7–9), respectively] and selected values of Knudsen number Kn_* . The outer boundary conditions for these functions have been established from the subsonic continuum solutions [see Eqs. (1–3) and (9)] at distances far behind the shock wave $r/R_a = 4$ and the various fixed values of the pressure ratio p_{0^*}/p_a . In particular, here we assume $f = f_a$, $T = T_a = 293$ K, and $n = n_a$, which corresponds to the selected value of the pressure ratio. The velocity u is calculated from the mass conservation principle $\rho_a u r^2 = \rho_* u_* r_*^2$. Initial state of the flow was a vacuum.

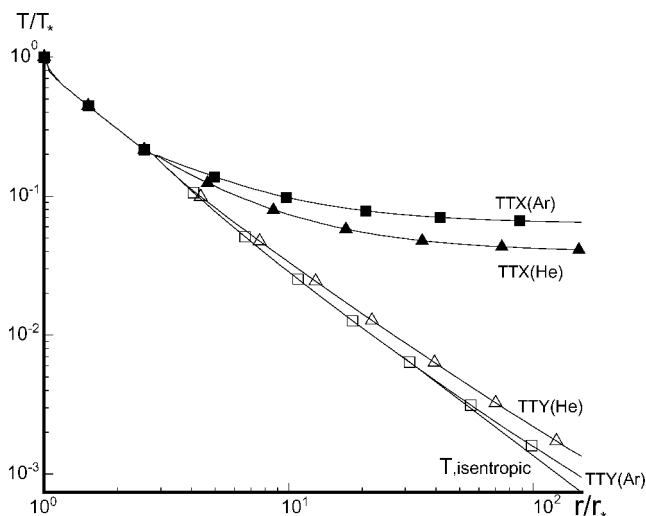
Code validation was established by using the methodology of Bird¹⁹ and Gimelshein et al.²⁸ The most important parameters of the kinetic approach (mesh size, number of simulating molecules, and time step) have been varied to obtain a reliable solution. The DSMC calculation of the spherically symmetrical flow was performed for four different sets of numerical parameters at Knudsen number $Kn_* = 0.015$, pressure ratio $p_{0^*}/p_a = 100$, and mole fraction of heavy component $f_* = 0.5$. The following values of the total number of cells and molecules were used for each set, respectively: 1) 1000 and 13,080; 2) 2000 and 25,380; 3) 4000 and 51,630; and 4) 10,000 and 109,720. Figures 1–3 show the calculated Mach number, number density, and mole fraction of argon, respectively, for the four different sets of parameters. The distributions of Mach number (see Fig. 1) and number density (see Fig. 2) are practically independent from the selected parameter sets. The sensitivity of the solution

of the mole fraction of argon (see Fig. 3) to the cell size and number of simulated molecules is significant in the area of the spherical shock wave. All three considered functions have matched the supersonic and subsonic continuum solutions (solid lines) outside the spherical shock wave at various parameter sets. The fourth DSMC parameter set is assumed to provide a result that is independent of both the number of molecules and the mesh size.

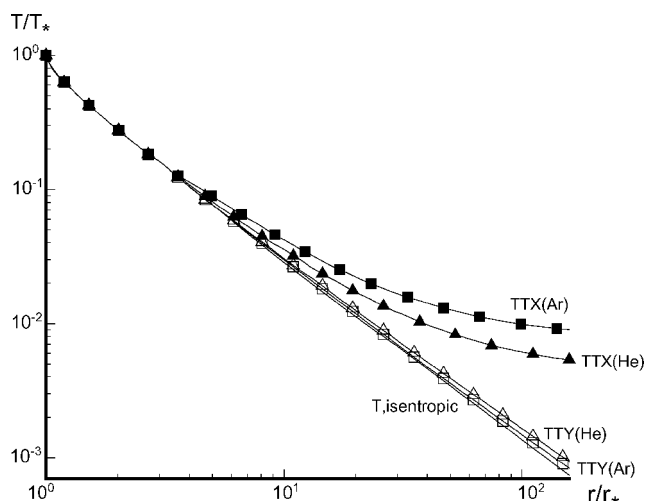
The cell geometry has been chosen to minimize the changes in the macroscopic properties (temperature, pressure, and density) across the individual cell.^{19,27} The variation in cell width has been based on the geometric progression principle¹⁹ and defined by the ratio $c = 20$ of the width of the cell adjacent to the outer boundary to the width of the cell adjacent to the inner boundary. In all cases the usual criterion¹⁹ for the time step Δt_m has been realized: $1 \times 10^{-10} \leq \Delta t_m \leq 1 \times 10^{-8}$ s. Under these conditions gasdynamic parameters are converged with respect to the time step. The ratio of the mean separation between collision partners to the local mean free path and the ratio of the time step to the local mean collision time have been well under unity over the flowfield.

Expansion of a Gas Mixture into a Vacuum

The DSMC results of the gas-mixture expansion (under the critical sonic conditions and the value of the argon mole fraction $f_{Ar,*} = 0.5$) from a spherical source into a vacuum (as the outer boundary) are shown in Fig. 4 for two values of the Knudsen number $Kn_* = 0.015$ (Reynolds number $Re_* = 124$) and 0.0015 ($Re_* = 1.24 \times 10^3$). The



a) $Kn_* = 0.015$



b) $Kn_* = 0.0015$

Fig. 4 Parallel (TXX) and transverse (TTY) temperature distributions in the spherical expansion of Ar-He mixture into vacuum.

major effect of freezing the parallel temperature can be observed. Bird¹⁹ and Cercignani²⁹ discussed the freezing effect for one-component gas in detail. The point of a very gradual rise of the parallel temperature above the continuum value is usually associated with the breakdown of continuum flow in expansions.¹⁹ The numerical results show that the freezing comes first for heavier molecules of argon at larger values of the Knudsen number (Fig. 4). The transverse temperature for both species follows the temperature in the isentropic expansion [see solutions (8) and (12)]. The mole fraction of species remains about constant, $f_{Ar} = 0.5$, along the streamlines.

Expansion of a Gas Mixture into a Flooded Space

The flow pattern is different in the case of gas-mixture expansion into a flooded space.^{8,9,24,25} The distributions of mole fraction of argon, pressure, stream and diffusion velocities, overall, species, parallel and transverse temperatures are shown in Figs. 5–12 at $Kn_* = 0.015$ and various pressure ratios $P = p_{0*}/p_a = 10^2, 10^3$, and 10^4 (filled squares, circles, and triangles, respectively). The results for $Kn_* = 0.0015$ and $p_{0*}/p_a = 10^4$ (diamonds) are also shown for comparison purposes.

It was found that the spherical flow could be separated by the coordinate $R_a = r_*(p_{0*}/p_a)^{1/2}$, introduced in Eq. (5), into two regions with significantly different properties. In the first “internal” region at $r < R_a$, the flow is supersonic [see Fig. 1, where the distribution of

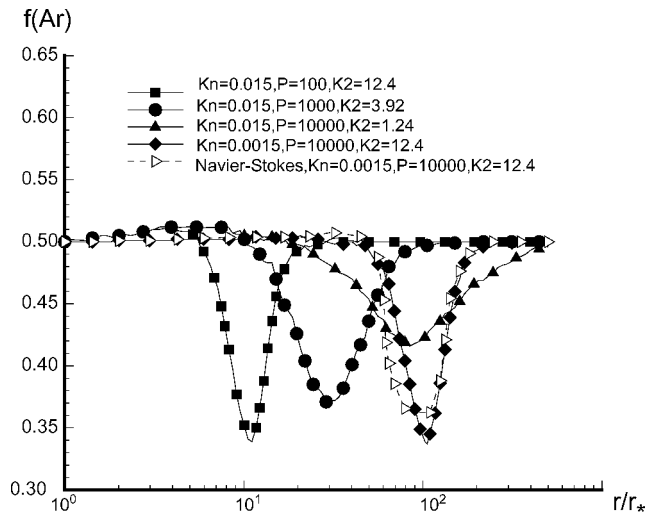


Fig. 5 Argon mole fraction distributions in spherical expanding flow at different Knudsen numbers Kn_* and pressure ratios P .

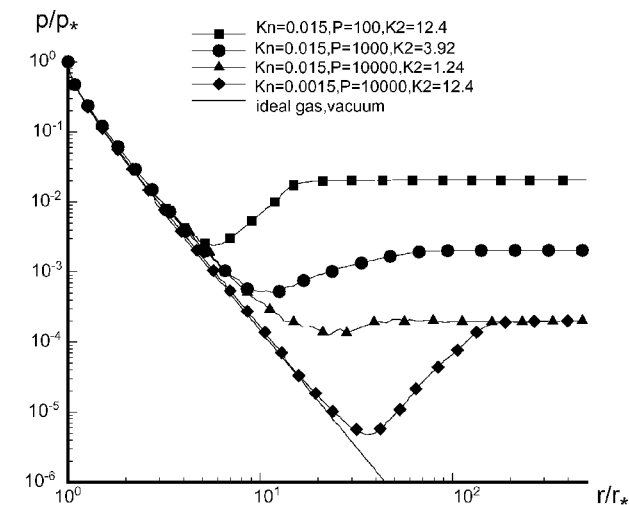


Fig. 6 Pressure in spherical expanding flow of Ar-He mixture at different Knudsen numbers Kn_* and pressure ratios P .

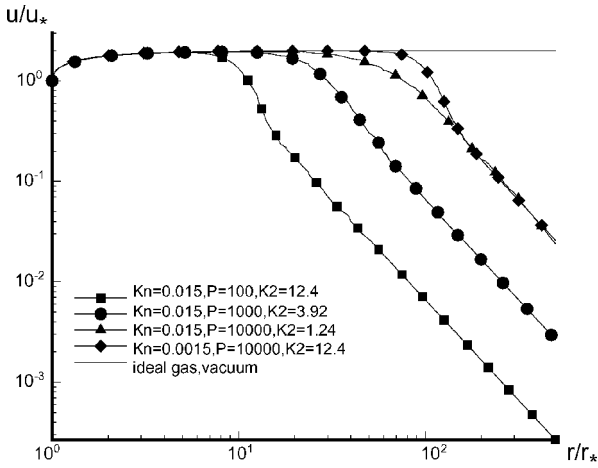


Fig. 7 Stream velocity in spherical expanding flow of Ar-He mixture at different Knudsen numbers Kn_* and pressure ratios P .

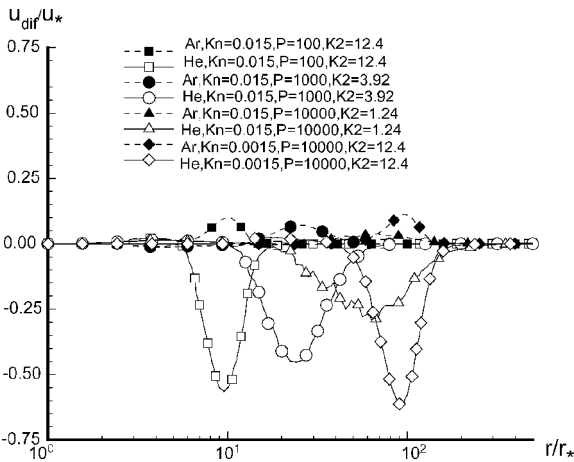


Fig. 8 Diffusion velocities of argon and helium in expanding flow of Ar-He mixture at different Knudsen numbers Kn_* and pressure ratios P .

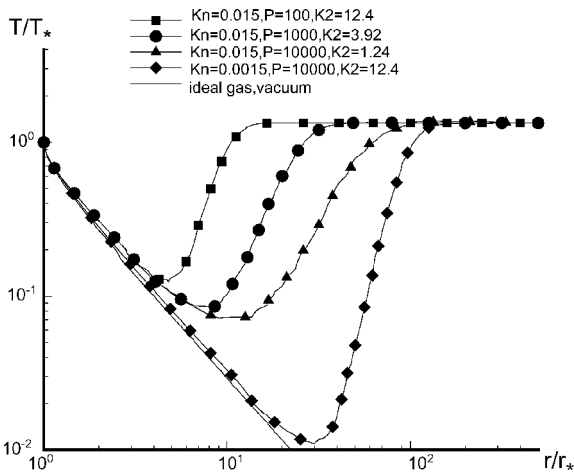


Fig. 9 Overall temperature in spherical expanding flow of Ar-He mixture at different Knudsen numbers Kn_* and pressure ratios P .

Mach number is presented at pressure ratio $p_{0*}/p_a = 100$, and the critical value of M occurs at distance $R_a/r_* = (p_{0*}/p_a)^{1/2} = 10$. The supersonic flow parameters depend on two similarity factors of Knudsen number Kn_* , based on the critical radius of a spherical source r_* , and pressure ratio $P = p_{0*}/p_a$ (or coordinate R_a). In the second “external” region at $r > R_a$ (see Figs. 1 and 5–12), there is a subsonic stream that is smoothly adapting to the ambient conditions at the infinity and depends on the Knudsen number Kn_a , based on the lengthscale parameter at infinity $L = (QU_a/4\pi\gamma p_a)^{1/2}$, which is

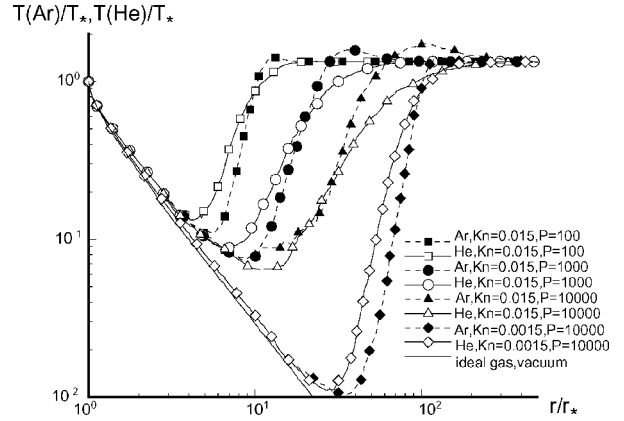


Fig. 10 Species temperatures in spherical expanding flow of Ar-He mixture at different Knudsen numbers Kn_* and pressure ratios P .

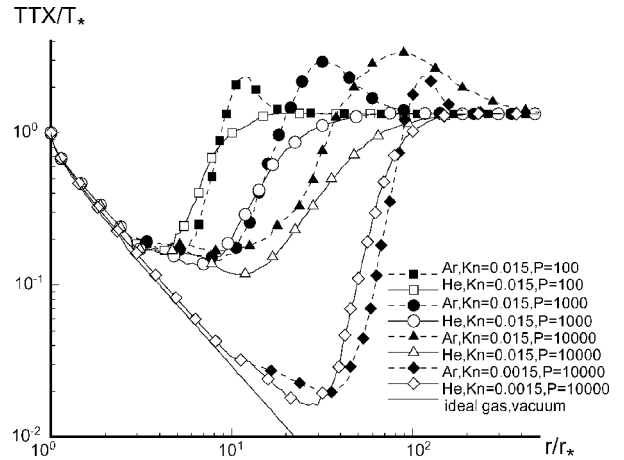


Fig. 11 Parallel temperatures of species in spherical expanding flows of Ar-He mixture at different Knudsen numbers Kn_* and pressure ratios P .

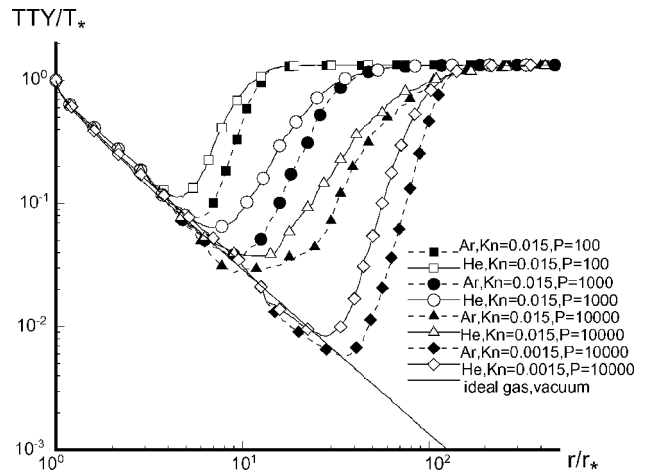


Fig. 12 Transverse temperatures of species in spherical expanding flows of Ar-He mixture at different Knudsen numbers Kn_* and pressure ratios P .

the major similarity parameter in the second region. The parameter L can be expressed as a multiple of R_a .

Using the definition of the overall mean free path^{18,19} for the mixture of the VHS molecules, the following correlation²⁰ between major similarity parameters (Kn_* and Kn_a) can be found:

$$\frac{Kn_a}{Kn_*} = \left(\frac{m_*}{m_a}\right)^{\frac{1}{4}} \left(\frac{T_a}{T_*}\right)^{s+\frac{1}{4}} \left(\frac{2}{\gamma+1}\right)^{\gamma/2(\gamma-1)} \sqrt{\frac{p_{0*}}{p_a}} \quad (19)$$

Another important similarity factor $K_2 = Re_*(p_{0*}/p_a)^{1/2} = Re_{Ra} \approx Re_{a,L}$ can be used to study the flow structure in the external region.^{3,21} For $K_2 = 12.4$ ($Kn_a = 0.17$) the concentration of argon changes insignificantly in the supersonic region at $r \ll R_a$ (Fig. 5). Because of the large gradients of the flow parameters in the shock-wave front (Figs. 6 and 9), the considerable increase in the velocity of the light helium component in this region is realized (Fig. 8). Accumulation of the light component occurs in the leading front of the spherical shock wave (Fig. 5), just as in the normal shock-wave case considered by Bird,¹⁹ Zeldovich and Raizer,³⁰ and Nagornykh.³¹ The enrichment of the mixture with the light component begins with an increase of pressure as it can be observed from comparison of distributions of mole fractions and pressure shown in Figs. 5 and 6, respectively. This fact indicates that baro-diffusion effects dominate in this part of the shock wave. The minimum value of the mole fraction of argon occurs at the location, where the positive pressure gradient is maximum. For near-continuum flow conditions at $K_2 = 12.4$, the DSMC data (diamonds) correlate with the solutions of the Navier–Stokes equations⁸ (shown as right-pointed open triangles in Fig. 5) at acceptable accuracy.

In all considered cases the hypersonic stream velocity is slightly different from the maximum speed of the isentropic inviscid flow [solutions (11)] (Fig. 7) and correlates well with the velocity predicted by the Navier–Stokes (continuum) approach (Fig. 1). The pressure ratio significantly influences the thickness of the spherical shock wave, which can be measured differently by using the distributions of the species concentration, pressure, diffusive velocities, and heavy-component parallel and transverse temperatures (Figs. 5, 6, 8, 11, and 12, respectively).

In contrast to the plane shock-wave studies,^{13–15,17–19,30,31} the methodology of measuring the thickness of the spherical shock wave is still under investigation. Here, the best candidate function is entropy [see Eq. (6) and discussion in Ref. 22]. Unfortunately, at this point the entropy-based parameter could not be developed from the available DSMC data.

With decreasing similarity rarefaction parameter K_2 , the flow pattern is changed dramatically in the shock wave and behind it. For transitional flow regime at $K_2 = 1.24$ ($Kn_a = 1.7$), the diffusion zone (marked by triangles in Figs. 5–12) is significantly wider than in the case with $K_2 = 12.4$ ($Kn_a = 0.17$) (squares and diamonds). In the region inside and behind the shock wave, a multitemperature regime of the flow is identified (Figs. 10–12). However, the significant enrichment of the mixture with the heavy component ($f_{Ar} \gg f_{Ar,a}$) inside the wave front at $K_2 = 1.24$, described by Gusev and Riabov⁸ by means of the continuum concept, was not observed. This fact indicates that the solutions⁸ of the Navier–Stokes equations are invalid at low values of the similarity rarefaction parameter K_2 that correspond to the high values of Knudsen numbers, $Kn_a > 1$.

In contrast to the one-temperature continuum approach,^{1,7,8} the DSMC method allows the simulation of the multitemperature kinetic media (Figs. 9–12). The most significant differences can be observed in distributions of parallel temperature of argon and helium across the spherical shock wave. The parallel temperature of argon has maximum at $r \approx R_a$, its maximum value increases with decreasing similarity rarefaction parameter K_2 (Fig. 11), and this value is larger the ambient gas stagnation temperature T_a by the factor of three at $K_2 = 1.24$ ($Kn_a = 1.7$). The parallel temperature of helium (see Fig. 11) and species transverse temperatures (Fig. 12) follow the classical temperature profile. In all considered cases of similarity parameters, helium temperatures increase more rapidly than argon ones in the supersonic part of the shock wave. The situation is reverse in the subsonic zone at $r > R_a$. The gap between species temperatures in this area increases with decreasing similarity rarefaction parameter K_2 (Figs. 10–12).

Similarity of Flows Behind the Spherical Shock Wave

Similarity analysis^{3,21} has been used to analyze the flow structure in the “external” region at $r > R_a$. The following dimensional parameters are used for normalization purposes: R_a , ρ_a , U_a , p_a , and T_a . In this case index a refers to the ambient medium conditions at infinity. The renormalized characteristics of the spherical

expanding flow in the external region are shown in Figs. 13–18. All considered flow characteristics (species concentration, pressure, stream and diffusion velocities, overall, species, parallel and transverse temperatures) correlate well in the region ($r \geq R_a$) at the same rarefaction parameters ($K_2 = 12.4$) and various internal parameters of the Knudsen number Kn_* .

In all considered cases, the stream velocity changes in accordance with the law $u \sim (r/R_a)^{-2}$ behind the shock wave (Fig. 15). At $r > 0.7R_a$ transverse temperatures of helium follow the overall temperature as shown in Fig. 18.

Expansion of Argon to Helium and Helium to Argon

The spherical expansion of a binary gas mixture into a flooded space has been analyzed in the case of the presence of a diffusive flux at the infinity $r \gg R_a$. The numerical results were calculated for the case of the expansion of argon with little helium content ($f_{Ar,*} = 0.99$) into a space filled by helium with a small admixture of argon ($f_{Ar,a} = 0.02$). The distributions of the argon concentration f_{Ar} , number density, and pressure related to this case with $Kn_* = 0.014$, $Re_* = 78.5$, and $K_2 = 0.785$ are presented in Fig. 19.

The other case of the expansion of helium with a little content of argon ($f_{Ar,*} = 0.011$) into a space filled by argon with small admixture of helium ($f_{Ar,a} = 0.9$) was also analyzed. The distributions of the argon concentration f_{Ar} , number density, and pressure in flow at $Kn_* = 0.03$, $Re_* = 453$, and $K_2 = 4.53$ are shown in Fig. 20.

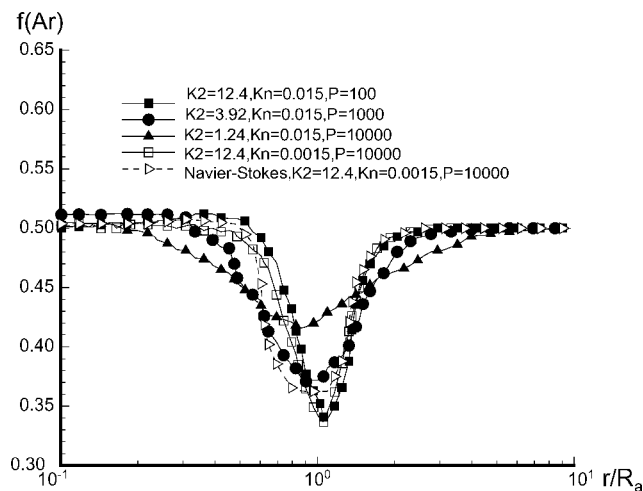


Fig. 13 Argon mole fraction distributions in a spherical shock wave at different values of rarefaction parameters K_2 and Kn_* .

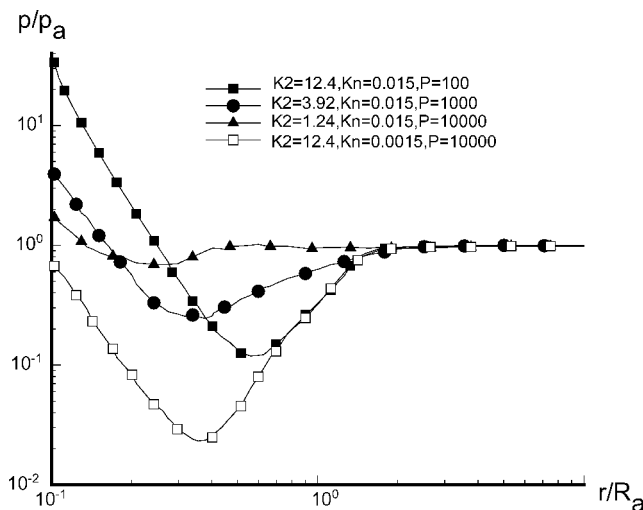


Fig. 14 Pressure in a spherical shock wave at different values of rarefaction parameters K_2 and Kn_* .

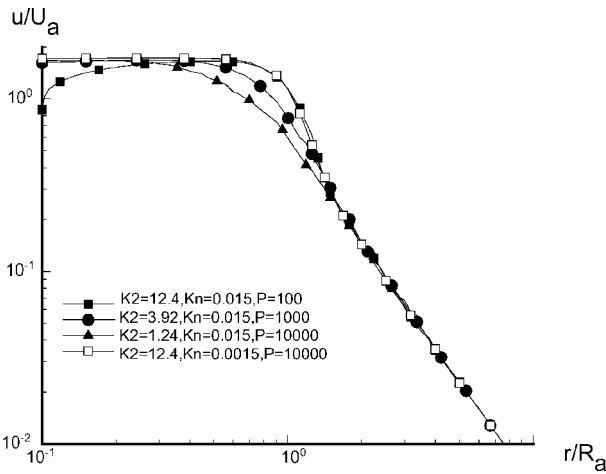


Fig. 15 Stream velocity of Ar-He mixture in a spherical shock wave at different values of rarefaction parameters K_2 and Kn_* .

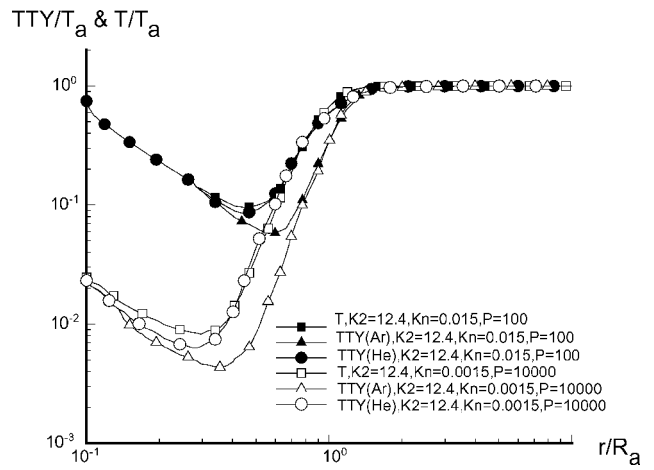


Fig. 18 Transverse temperature of argon and helium in spherical shock waves at $K_2 = 12.4$ and $Kn_* = 0.015$ and 0.0015 .

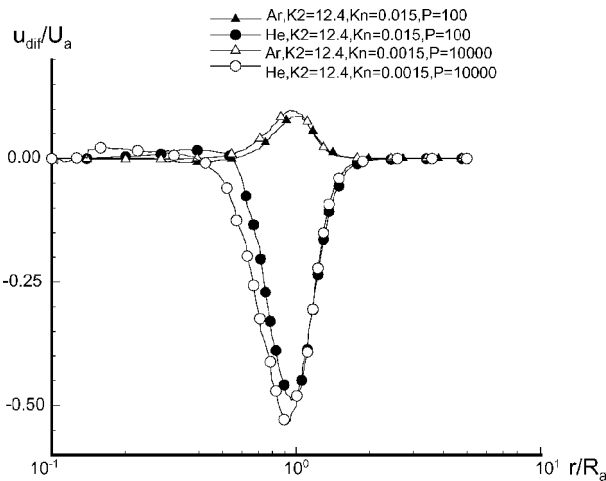


Fig. 16 Diffusion velocities of argon and helium in a spherical shock wave at $K_2 = 12.4$ and $Kn_* = 0.015$ and 0.0015 .

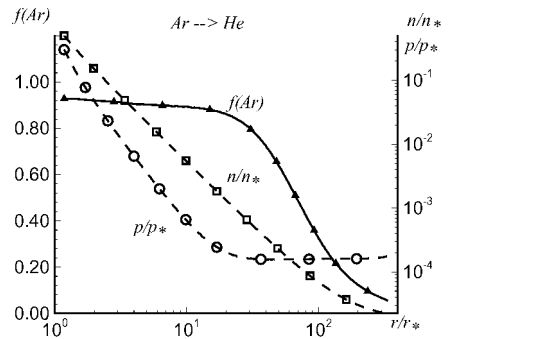


Fig. 19 Argon mole fraction, pressure, and number density in expansion of argon into helium at $Kn_* = 0.014$ and $K_2 = 0.785$.

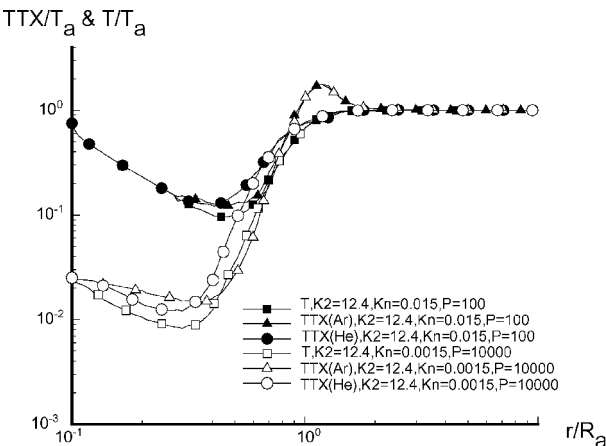


Fig. 17 Parallel temperature of argon and helium in a spherical shock wave at $K_2 = 12.4$ and $Kn_* = 0.015$ and 0.0015 .

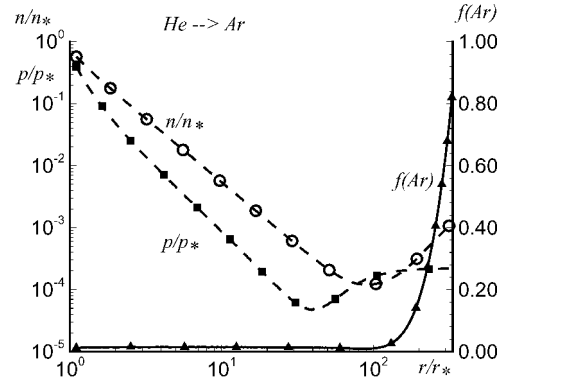


Fig. 20 Argon mole fraction, pressure, and number density in expansion of helium into argon at $Kn_* = 0.003$ and $K_2 = 4.53$.

Conclusions

The results demonstrate that in both cases the background gas does not penetrate through the shock wave into the inner supersonic region of the flow. This property was noted in experiments of Skovorodko and Chekmarev.⁷ In the considered cases the continuum approach is not applicable in the flow area behind the shock waves. The discussed phenomena and the results of previous studies^{8,9} were used for estimating the flow parameters and the axisymmetric jet structure in various aerodynamic applications.⁹

The direct simulation Monte Carlo and similarity methods have been used in the studies of kinetic and gasdynamic effects in the expanding flows of the argon-helium mixture from a spherical source at sonic conditions. The diffusive effects are significant for estimation of the shock-wave width, the effectiveness of species separation, and ambient gas penetration. The group of similarity parameters (Kn_* , Kn_a , K_2 , Re_* , and Re_a) was found to identify the rarefaction flow regimes. The kinetic effects play a significant role in freezing the parallel temperature of the species in the hypersonic zone; in enriching flow with the light (helium) component in the spherical shock wave (with the maximum enrichment on the sonic surface inside the wave at $r = R_a$), and in abnormally increasing the parallel temperature of the heavier (argon) component in the vicinity of the sonic surface inside the shock wave. The rarefaction parameter K_2

is the major criterion for simulating flows in this area. The problem of an accurate definition of spherical shock-wave thickness will be addressed in the future study.

References

- ¹Sherman, F. S., "Hydrodynamical Theory of Diffusive Separation of Mixture in a Free Jet," *Physics of Fluids*, Vol. 9, No. 5, 1965, pp. 773–779.
- ²Gusev, V. N., and Klimova, T. V., "Flow in Underexpanded Nozzle Jets," *Fluid Dynamics*, Vol. 3, No. 4, 1968, pp. 121–125.
- ³Gusev, V. N., Klimova, T. V., and Riabov, V. V., "Similarity of Flows in Strongly Underexpanded Jets of Viscous Gas," *Fluid Dynamics*, Vol. 13, No. 6, 1978, pp. 886–893.
- ⁴Bochkarev, A. A., Kosinov, V. A., Prikhodko, V. G., and Rebrov, A. K., "The Flow of a Rarefied Gaseous Mixture from an Orifice," *Journal of Engineering Physics*, Vol. 18, No. 4, 1970, pp. 444–450.
- ⁵Bochkarev, A. A., Kosinov, V. A., Prikhodko, V. G., and Rebrov, A. K., "The Structure of Supersonic Jet of Argon–Helium Mixture in Vacuum," *Journal of Applied Mechanics and Technical Physics*, Vol. 11, No. 5, 1970, pp. 857–861.
- ⁶Brook, J. W., Hamel, B. B., and Muntz, E. P., "Theoretical and Experimental Study of Background Gas Penetration into Underexpanded Free Jets," *Physics of Fluids*, Vol. 18, No. 5, 1975, pp. 517–528.
- ⁷Skovorodko, P. A., and Chekmarev, S. F., "On the Gas Diffusion in a Low Density Jet," *Rarefied Gas Dynamics*, edited by S. S. Kutateladze and A. K. Rebrov, Inst. of Thermophysics, Novosibirsk, Russia, 1976, pp. 68–76 (in Russian).
- ⁸Gusev, V. N., and Riabov, V. V., "Spherical Expansion of a Binary Gas Mixture into a Flooded Space," *Fluid Dynamics*, Vol. 13, No. 2, 1978, pp. 249–256.
- ⁹Riabov, V. V., "Aerodynamic Applications of Underexpanded Hypersonic Viscous Jets," *Journal of Aircraft*, Vol. 32, No. 3, 1995, pp. 471–479.
- ¹⁰Rothe, D. E., "Electron Beam Studies of the Diffusive Separation of Helium–Argon Mixtures," *Physics of Fluids*, Vol. 9, No. 9, 1966, pp. 1643–1658.
- ¹¹Bochkarev, A. A., Kosinov, V. A., Prikhodko, V. G., and Rebrov, A. K., "Effect of Diffusion Separation When Hypersonic Flows of Rarefied Gas Mixture Collide," *Journal of Applied Mechanics and Technical Physics*, Vol. 12, No. 2, 1971, pp. 313–317.
- ¹²Center, R. E., "Measurement of Shock Wave Structure in Helium–Argon Mixtures," *Physics of Fluids*, Vol. 10, No. 8, 1967, pp. 1777–1784.
- ¹³Abe, J., and Oguchi, H., "Shock Wave Structure in Gas Mixtures," *Proceedings of the 6th International Symposium on Rarefied Gas Dynamics*, Vol. 1, edited by L. L. Trilling, Academic Press, New York, 1969, pp. 425–432.
- ¹⁴Harnet, L. N., and Muntz, E. P., "Experimental Investigation of Normal Shock Wave Velocity Distribution Function in Mixtures of Argon and Helium," *Physics of Fluids*, Vol. 15, No. 4, 1972, pp. 565–572.
- ¹⁵Bochkarev, A. A., Rebrov, A. K., and Timoshenko, N. I., "The Shock Wave Structure in the Ar–He Mixture," *Izvestiya Sibirskogo Otdeleniya AN SSSR, Seria Tekhnicheskikh Nauk*, Vol. 1, No. 3, 1976, pp. 96–104 (in Russian).
- ¹⁶Bochkarev, A. A., and Prikhodko, V. G., "The Comparison of Supersonic Flow Field Structure About a Sphere in Nitrogen and Nitrogen–Hydrogen Mixture," *Trudy IV Vsesoyuznoi Konferentsii po Dinamike Razrezhennogo Gaza I Molekularnoi Gazovoi Dinamike*, Central Aerohydrodynamics Institute (TsAGI), Moscow, 1977, pp. 621–627 (in Russian).
- ¹⁷Bird, G. A., "The Structure of Normal Shock Wave in Binary Gas Mixture," *Journal of Fluid Mechanics*, Vol. 31, Pt. 4, March 1968, pp. 657–668.
- ¹⁸Bird, G. A., *Molecular Gas Dynamics*, Oxford Univ. Press, London, 1976, pp. 143–171.
- ¹⁹Bird, G. A., *Molecular Gas Dynamics and the Direct Simulation of Gas Flows*, Oxford Univ. Press, London, 1994, pp. 282–305.
- ²⁰Riabov, V. V., "Numerical Analysis of Compression and Expansion Binary Gas–Mixture Flows," AIAA Paper 96-0109, Jan. 1996.
- ²¹Gusev, V. N., and Mikhailov, V. V., "Similarity of Flows with Expanding Jets," *Uchenyye Zapiski TsAGI*, Vol. 1, No. 4, 1970, pp. 22–25 (in Russian).
- ²²Anderson, J. D., Jr., *Modern Compressible Flow*, McGraw–Hill, New York, 1990, p. 71.
- ²³Chapman, S., and Cowling, T. G., *The Mathematical Theory of Non-Uniform Gases*, 3rd ed., Cambridge Univ. Press, London, 1970, pp. 165–183.
- ²⁴Gusev, V. N., and Zhabkova, A. V., "The Flow of a Viscous Heat-Conducting Compressible Fluid into a Constant Pressure Medium," *Proceedings of the 6th International Symposium on Rarefied Gas Dynamics*, Vol. 1, edited by L. L. Trilling, Academic Press, New York, 1969, pp. 847–855.
- ²⁵Gusev, V. N., and Zhabkova, A. V., "Properties of the Spherical Expansion of a Viscous Gas into a Flooded Space," *Uchenyye Zapiski TsAGI*, Vol. 7, No. 4, 1976, pp. 42–50 (in Russian).
- ²⁶Freeman, N. C., and Kumar, S., "On the Solution of the Navier–Stokes Equations for a Spherically Symmetric Expanding Flow," *Journal of Fluid Mechanics*, Vol. 56, Pt. 3, 1972, pp. 523–532.
- ²⁷Bird, G. A., "Monte-Carlo Simulation in an Engineering Context," *Rarefied Gas Dynamics*, edited by S. S. Fisher, Vol. 74, Progress in Astronautics and Aeronautics, AIAA, New York, 1981, pp. 239–255.
- ²⁸Gimelshein, S. F., Alexeenko, A. A., and Levin, D. A., "Modeling of the Interaction of a Side Jet with a Rarefied Atmosphere," *Journal of Spacecraft and Rockets*, Vol. 39, No. 2, 2002, pp. 168–176.
- ²⁹Cercignani, C., *Rarefied Gas Dynamics: From Basic Concepts to Actual Calculations*, Cambridge Univ. Press, Cambridge, England, U.K., 2000, pp. 194–199.
- ³⁰Zeldovich, Ya. B., and Raizer, Yu. P., *Physics of Shock Waves and High-Temperature Hydrodynamic Phenomena*, Vol. 2, Academic Press, New York, 1967, pp. 465–488.
- ³¹Nagornyykh, Yu. D., "Flow of a Mixture of Light and Heavy Gases Behind a Spherical Shock Wave," *Gas Dynamics and Physical Kinetics*, Nauka, Novosibirsk, Russia, 1974, pp. 24–29 (in Russian).